MINISTRY OF INDUSTRY AND TRADE MINISTRY OF EDUCATION AND TRAINING

NATIONAL RESEARCH INSTITUTE OF MECHANICAL ENGINEERING

NARIME

HOANG ANH TOAN

INVESTIGATION INTO THE EFFECTS OF TECHNOLOGICAL PARAMETERS ON PRODUCTIVITY AND QUALITY IN EXTERNAL CYLINDRICAL HARD MILLING USING MINIMUM QUANTITY LUBRICATION WITH CuO NANOPARTICLES

Major: Mechanical Engineering

Code: 9520103

SUMMARY OF DOCTORAL DISSERTATION

Ha Noi - 2026

The work was carried out at the Research Institute of Mechanical Engineering, Ministry of Industry and Trade.

Scientific Supervisors:

1. Prof. Dr. Vu Ngoc Pi
2. Assoc. Prof. Dr. Hoang Van Got

Reviewer 1:

Reviewer 2:

Reviewer 3:

The doctoral dissertation will be defended before the Institute-level Doctoral Dissertation Evaluation Council.

Venue: Research Institute of Mechanical Engineering – Ministry of Industry and Trade

Room 209, Main Headquarters Building, No. 4 Pham Van Dong Street, Cau Giay District, Hanoi, Vietnam.

At …… hours …… minutes, on …… day …… month …… 2026.

The dissertation is available for consultation at the following libraries:

- Library of the Research Institute of Mechanical Engineering, No. 4 Pham Van Dong Street, Cau Giay District, Hanoi, Vietnam.
- National Library of Vietnam.

LIST OF PUBLICATIONS RELATED TO THE DISSERTATION RESEARCH

1. Dinh Van Thanh, Hoang Van Got, Vu Ngoc Pi, Do The Vinh, and **Hoang Anh Toan*.**"Response Surface Modeling and Optimization of Cutting Force in External Cylindrical Hard Milling of 90CrSi Tool Steel under CuO Nano-MQL". WSEAS Transactions on Applied and Theoretical Mechanics (Scopus Q3). Accepted for publication, November 2025.

2. Tran Quoc Hung, Hoang Van Got, Do The Vinh, Vu Ngoc Pi, and **Hoang Anh Toan*.**"Surface Roughness Modeling and Parameter Influence in Nano-MQL Milling Process". Journal of Mechanical Engineering of Vietnam, No. 329, June 2025, ISSN 2615-9910 (print), ISSN 2815-5505 (online).

3. Luu Anh Tung, Hoang Van Got, Do The Vinh, Vu Ngoc Pi, and **Hoang Anh Toan*.**"MRR Optimization in Nano-MQL Milling of Hardened 90CrSi Tool Steel Using CuO Nanoparticles". Journal of Mechanical Engineering of Vietnam, No. 329, June 2025, ISSN 2615-9910 (print), ISSN 2815-5505 (online).

4. Toan Hoang Anh, Thanh Dinh Van, Got Hoang Van, Vinh Do The, and Pi Vu Ngoc."Statistical Modeling and Optimization of Surface Roughness in Nano-MQL Milling of Hardened 90CrSi Cylindrical Surfaces". In: Proceedings of the International Conference on Engineering Research and Applications (ICERA 2025), December 2025 (Scopus Q4). (International conference paper).

5. Toan Hoang Anh, Got Hoang Van, Vinh Do The, Pi Vu Ngoc, and Thanh Dinh Van."Enhanced MRR in Hard Milling Using CuO Nano-Lubricants: Experimental and RSM-Based Modeling Study". In: Proceedings of the International Conference on Engineering Research and Applications (ICERA 2025), December 2025 (Scopus Q4). (International conference paper).

6. Nguyen Anh Tuan, Hoang Van Got, Do The Vinh, Vu Ngoc Pi, Hoang Anh Toan*."Pareto-Based Multi-Objective Optimization and Trade Off Analysis of Material Removal Rate and Surface Roughness in CuO Nano-MQL Hard Milling of 90CrSi Tool Steel". In: Proceedings of the International Conference on Engineering Research and Applications (ICERA 2026), 2026 (Scopus Q4). (International conference paper).

7. Nguyen Anh Tuan, Hoang Van Got, Do The Vinh, Vu Ngoc Pi, Hoang Anh Toan*."Multi-Objective Optimization of Hard Milling of Hardened 90CrSi Tool Steel under CuO Nano-MQL Using Gaussian Process Regression and NSGA-II".In: Proceedings of the International Conference on Engineering Research and Applications (ICERA 2026), 2026 (Scopus Q4). (International conference paper).

INTRODUCTION

1. Research Necessity

Convex shaped cylindrical surfaces are widely used in the manufacturing of punches and dies. Although traditional grinding achieves high accuracy, it incurs significant costs, low productivity, and limited flexibility. To replace the grinding operation, CNC hard milling of hardened materials offers a promising direction to streamline manufacturing processes and enhance production flexibility. However, hard milling of 90CrSi tool steel presents major challenges due to high cutting forces and temperatures, causing rapid tool wear. Conventional flood cooling is ineffective and susceptible to thermal shock, leading to insert fracture. Consequently, nano-MQL minimum quantity lubrication technology combined with CuO nanoparticles is proposed as an alternative. To date, no systematic research exists on hard milling of hardened 90CrSi shaped cylindrical surfaces using nano-MQL. Therefore, the topic "Investigation into the effects of technological parameters on productivity and quality in external cylindrical hard milling using minimum quantity lubrication with CuO nanoparticles" possesses high necessity, addressing a scientific gap and fulfilling practical requirements in precision mechanical engineering.

2. Research Objectives

The overall objective of the dissertation is to enhance the performance of external cylindrical hard milling of 90CrSi steel by integrating nano-MQL technology with modern modeling and optimization methodologies.

Specific objectives include:

- Establishing an experimental database to support process analysis;
- Elucidating the effects of technological parameters on surface roughness, material removal rate, and cutting force;
- Developing predictive models using RSM and GPR methods;
- Executing single-objective and multi-objective optimization to determine optimal cutting regimes;
- Proposing a balanced machining regime applicable to industrial production.

3. Objects and Scope of Research

The research object of this dissertation is the external cylindrical hard milling process of 90CrSi steel on a CNC milling machine under nano-MQL cooling–lubrication conditions using CuO nanoparticles.

The research scope encompasses:

Workpiece material: Heat-treated 90CrSi steel (hard milling region).

Surface geometry: Shaped external cylindrical surfaces.

Cooling–lubrication technology: nano-MQL with CuO nanoparticles.

Evaluation indicators: Surface roughness (Ra), material removal rate (MRR, g/min), and resultant cutting force (F).

4. Research Methodology

The dissertation employs an integrated research methodology combining theoretical and experimental approaches to analyze, model, and improve the hard milling process of 90CrSi steel shaped cylindrical surfaces on CNC milling machines under nano-MQL conditions using CuO nanoparticles.

4.1. Theoretical Method

The theoretical method is applied to establish the scientific foundation for the study, including analyzing the hard milling mechanism and modeling the relationships between technological parameters and output quantities. The RSM model is utilized to predict surface roughness, material removal rate, and cutting force. On this basis, single-objective and multi-objective optimization problems are solved using the NSGA-II algorithm, combined with the AHP method and Knee point to select the overall optimal machining regime.

4.2. Experimental Method

The experimental method is implemented to build datasets and validate theoretical models. Hard milling experiments were conducted on a CNC milling machine equipped with a nano-MQL system using CuO nanoparticles and nano-composite coated solid carbide end mills. Output parameters including surface roughness, material removal rate, and resultant cutting force were measured using specialized equipment. Experimental results were statistically processed and utilized for model construction and validation testing of optimal cutting regimes.

5. Scientific Significance and Practical Significance

5.1. Scientific Significance

The dissertation contributes to clarifying the influence mechanism of technological parameters and nano-MQL conditions on the hard milling efficiency of 90CrSi steel when using nano-composite coated carbide end mills. Furthermore, the dissertation proposes an integrated method framework of RSM – GPR – NSGA-II – AHP for multi-objective optimization, contributing methodologically to precision mechanical machining.

5.2. Practical Significance of the Research

The research findings provide a scientific basis for selecting appropriate hard milling regimes for 90CrSi steel shaped cylindrical surfaces when using nano-composite coated carbide end mills in industrial production. The proposed multi-objective optimal machining regime helps balance surface quality and productivity while reducing cutting forces, contributing to enhanced economic efficiency and manufacturing sustainability.

6. New Contributions of the Dissertation

- A systematic study on the hard milling process of 90CrSi steel external cylindrical surfaces using 6-flute nano-composite coated carbide end mills under nano-MQL conditions with CuO nanoparticles.
- Construction of RSM models for predicting Ra, MRR, and F.
- Application of NSGA-II combined with GPR for multi-objective optimization of the hard milling process.
- Combination of the AHP method and Knee point to select the overall optimal machining regime.
- Proposal of a balanced machining regime verified through experimental validation.
- Application of multi-criteria decision-making methods TOPSIS, MARCOS, and EAMR to select the optimal solution from the feasible Pareto set.

7. Dissertation Structure

In addition to the Introduction and Conclusions & Recommendations, the dissertation consists of 5 chapters:

Chapter 1: Overview of hard milling, minimum quantity lubrication, and optimization.

Chapter 2: Theoretical background of hard milling, modeling, and optimization.

Chapter 3: Development of the experimental system.

Chapter 4: Experimental results and modeling of external cylindrical hard milling of 90CrSi steel under Nano-MQL conditions using CuO nanoparticles.

Chapter 5: Optimization of external cylindrical hard milling of 90CrSi steel under Nano-MQL conditions using CuO nanoparticles.

CHAPTER 1: OVERVIEW OF HARD MILLING, MINIMUM QUANTITY LUBRICATION, AND OPTIMIZATION

1.1. Introduction to Hard Milling

Hard milling is an advanced machining technique widely utilized in die and mold manufacturing and precision engineering domains. It refers to the process of cutting materials after heat treatment with a typical hardness ranging from 45 to 70 HRC, aimed at semi-finishing or finishing complex surfaces with demanding requirements for accuracy and smooth surface finish.



***Figure 1.2**. Mobile phone mold created by hard milling and the utilized hard milling parameters*

When compared to other finishing methods such as grinding and EDM, hard milling exhibits distinct advantages and disadvantages. The primary advantage of hard milling lies in its ability to flexibly produce complex 3D surfaces on CNC milling machines within a single setup, substantially shortening the manufacturing cycle and mitigating accumulated setup errors. The material removal rate (MRR) of hard milling is also significantly higher than that of grinding and EDM.

1.2. Introduction to Minimum Quantity Lubrication and Nano-MQL

1.2.1. Principles and Effectiveness of MQL Technology

Comprehensive studies demonstrate that minimum quantity lubrication (MQL) is an effective alternative to traditional flood cooling in machining, reducing cutting fluid consumption while simultaneously enhancing technological performance. As illustrated in Figure 1.4, the MQL system operates by delivering a minute quantity of lubricant mist into the cutting zone using high-pressure compressed air, enabling direct lubricant penetration into the tool-chip interface. Through this mechanism, MQL ensures cooling functions and provides superior lubrication compared to dry machining conditions.

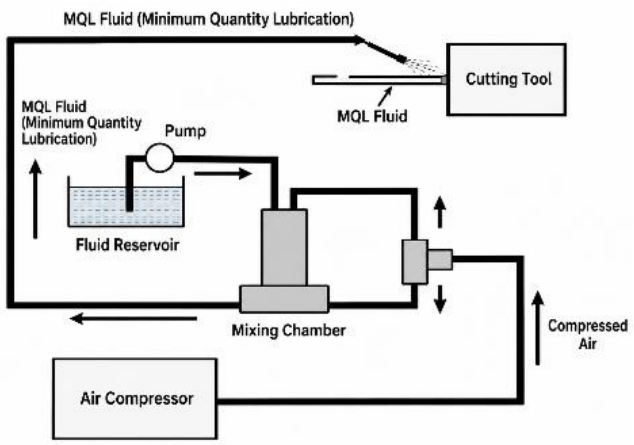


Figure 1.4. Schematic diagram of minimum quantity lubrication (MQL) system, wherein lubricant fluid is mixed with compressed air and delivered as a fine mist into the cutting zone to enhance cooling and lubrication performance.

1.2.2. Nano-MQL and the Special Role of CuO Nanoparticles

To address limitations regarding cooling and lubrication capabilities in conventional MQL, nanoparticle-enhanced minimum quantity lubrication (nano-MQL) has emerged as an effective approach to improve machining performance, particularly under hard machining conditions and difficult-to-cut materials.

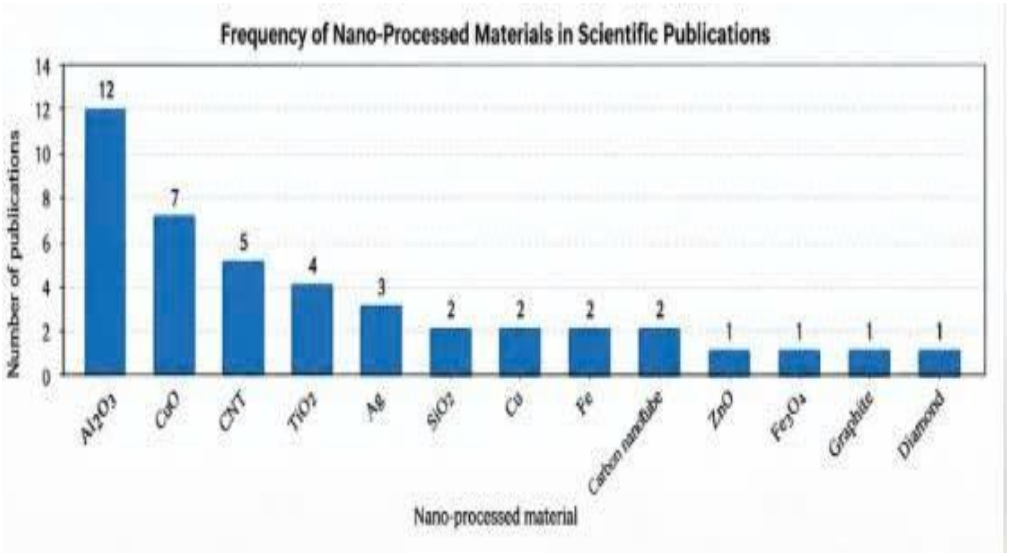


Figure 1.10. Ranking of nanoparticle types according to research frequency in nanofluid publications [28]

1.3. Research Studies on Modeling and Optimization in Hard Milling

1.3.1. Research Studies on Hard Milling Process Modeling

Overall, research in hard milling process modeling has achieved major advances, ranging from basic empirical models to complex numerical formulations and modern machine learning approaches. Nonetheless, research gaps persist regarding integrated multi-objective predictive models tailored for advanced machining environments like nano-MQL, especially for difficult-to-cut alloys under realistic manufacturing conditions.

1.3.2. Single-Objective Optimization in Hard Milling Machining

Single-objective optimization represents a widely adopted methodology in hard milling literature, where a single primary output response such as surface roughness, cutting force, tool wear, or productivity is designated as the target objective function for optimization.

1.3.3. Multi-Objective Optimization in Hard Milling Machining

In practical hard milling scenarios, technological targets such as surface finish, cutting force, tool wear, material removal rate (MRR), and energy consumption typically exhibit conflicting relationships. Consequently, multi-objective optimization becomes essential to establish an optimal compromise among these criteria. Unlike single-objective optimization, multi-objective optimization determines a Pareto optimal set, wherein no individual solution strictly dominates another across all objective functions.

1.4. Cutting Tool Materials in Hard Machining

Cutting tool materials play a decisive role in governing process stability and overall performance in hard machining. Current development trends focus on simultaneous optimization of substrate material and nano-coatings to achieve a balance between hardness, adhesion, and thermal stability, combined with advanced lubrication strategies towards efficient and sustainable machining.

1.5. Status of Hard Milling Research in Vietnam

In recent years, research on hard milling in Vietnam has developed significantly, reflected in both publication quantity and depth of content. Primary research directions focus on: evaluating the effects of technological parameters on surface quality, cutting forces, and tool wear;

A prominent research stream involves assessing cutting parameter effects on surface quality and forces during the milling of hardened steel. However, research regarding other material systems, tool coatings, high-accuracy non-linear predictive models, as well as machine learning integration with multi-objective optimization under nano-MQL conditions remains limited. This serves as an important rationale to extend investigations towards deeper and modern methodologies in the future.

1.6. Research Gaps

It is evident that an integrated research direction needs to be developed, focusing on: (i) experimental study of hard milling 90CrSi steel on external shaped cylindrical surfaces; (ii) systematic evaluation of nano-MQL effects using CuO nanoparticles on machining performance; and (iii) construction of predictive and multi-objective optimization models to determine optimal cutting conditions for industrial implementation. This represents a research trajectory with significant scientific and practical value, filling current gaps in hard milling literature.

Summary of Chapter 1

In Vietnam, hard milling research has made notable progress in experimental testing and MQL/nano-MQL applications, but remains limited in material scope, surface geometry, and modeling-optimization integration. From the literature review, four major research gaps are identified: (i) lack of hard milling studies on 90CrSi steel shaped external cylindrical surfaces; (ii) absence of systematic evaluation regarding nano-MQL (CuO) influence; (iii) lack of integrated models predicting surface roughness, cutting force, and MRR simultaneously; (iv) limited adoption of machine-learning-assisted multi-objective optimization.

On this foundation, the dissertation aims to conduct experimental research and establish predictive-optimization models for external cylindrical hard milling of 90CrSi steel under nano-MQL (CuO) conditions. This work elucidates technological mechanisms while delivering practical optimization solutions for modern mechanical manufacturing.

CHAPTER 2: THEORETICAL BACKGROUND OF HARD MILLING, MODELING, AND OPTIMIZATION

2.1. Theoretical Background of Hard Milling

2.1.1. Chip Formation Mechanism in Hard Milling

In hard milling, chip formation is governed simultaneously by high workpiece hardness, elevated strain rates in the cutting zone, and intermittent cutting characteristics per tooth. For hardened steels such as 90CrSi, SKD11, or wear-resistant steel HARDOX 500, high flow stress reduces uniform plastic deformation. Consequently, continuous stable chips are rarely generated; instead, localized deformation and shear localization occur, forming serrated chips.

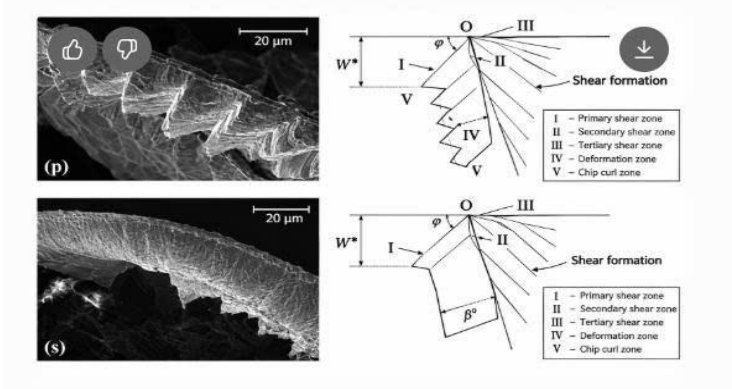


Figure 2.1: Chip morphology obtained during high-speed milling of hardened steel: (a) continuous chip with uniform deformation; (b) serrated chip with localized shear bands, indicating morphology transition with increasing cutting speed [1]

2.1.2. Heat Generation Mechanism and Thermo-Mechanical Behavior of Materials

2.1.2.1. Thermo-Mechanical Behavior of Materials

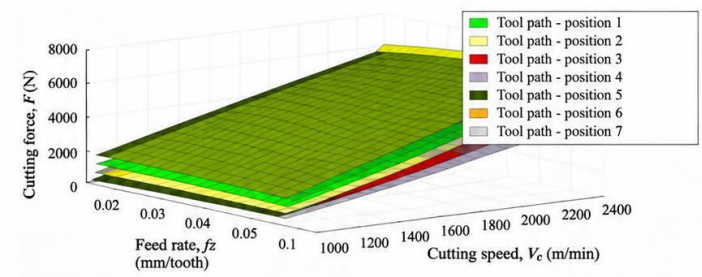


Figure 2.3. Stress-strain-temperature surface comparing material parameter sets .

2.1.2.2. Thermo-Mechanical Simulation via Finite Element Method

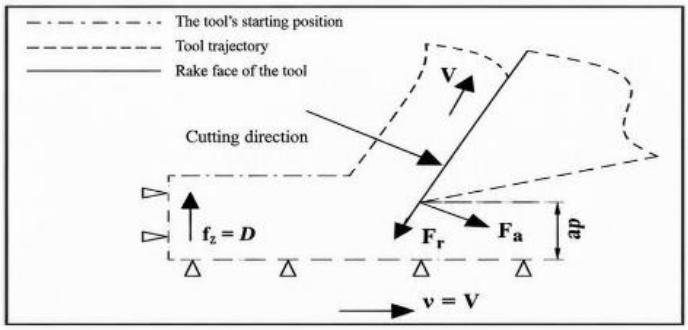


Figure 2.8: Thermo-mechanical boundary conditions in finite element simulation of hard milling

2.1.3. Friction Mechanisms in Hard Milling

Friction is one of the primary tribological phenomena in hard milling, developing at contact interfaces between the tool, chip, and machined surface. Serving as a major heat source at secondary shear zones and flank contact faces, friction directly impacts cutting forces, tool wear, surface roughness, and tool life.

2.1.3.1. Primary Frictional Contact Zones in Hard Milling

2.1.3.1.1. Tool Rake Face Friction

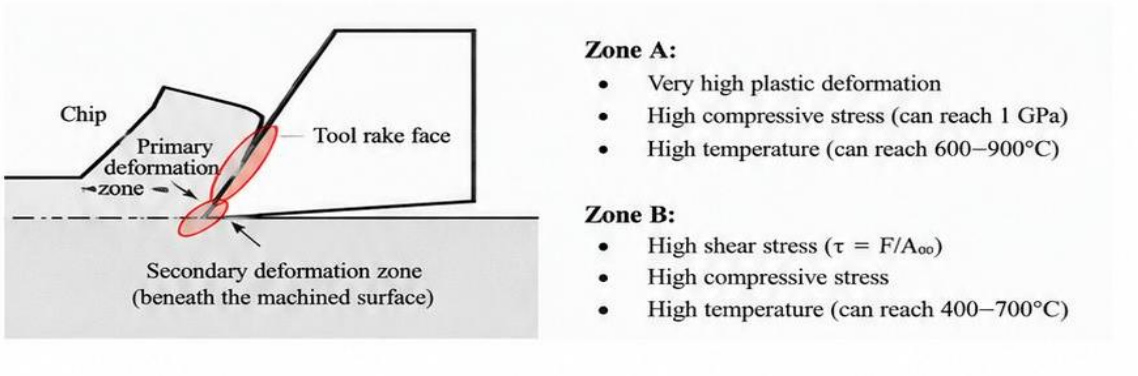


Figure 2.11. Model dividing tool-chip interface into two distinct contact zones

2.1.3.1.2. Tool Flank Face Friction

Flank face friction arises between the tool flank and freshly machined surface. Although heat generated here is lower than at the tool-chip zone, flank friction directly dictates surface roughness and dimensional accuracy. As flank wear progresses, expanded contact area increases frictional forces, causing plowing and localized plastic deformation on the surface layer.

2.1.4. Tool Wear Mechanisms in Hard Milling

Tool wear represents a primary driver of productivity degradation, dimensional error, and poor surface finish in hard milling. Because cutting occurs under heavy mechanical loads, elevated temperatures, and severe friction regimes, cutting tools simultaneously experience multiple wear mechanisms.

2.1.5. Performance Evaluation Indicators for Hard Milling

Hard milling performance is typically assessed using key indicators including surface roughness (Ra), cutting force (F), and material removal rate (MRR).

2.2. Cooling and Lubrication Methods in Hard Milling

2.2.1. Dry Machining

Dry machining avoids using cutting fluids during processing. It represents a key vector towards sustainable manufacturing by eliminating coolant costs, reducing environmental impacts, and improving workplace safety.

2.2.2. Flood Cooling Lubrication (Flood Cooling)

Flood cooling is a traditional method delivering high fluid flow continuously to the cutting zone to fulfill cooling, lubrication, and chip flushing. Leveraging high heat capacity, it controls temperatures and tool overheating, enhancing tool life.

2.2.3. Minimum Quantity Lubrication (MQL)

MQL bridges dry and flood machining, delivering minute oil aerosol quantities (10–50 mL/h) via compressed air stream directly into the cutting zone. The system relies on optimized lubricant parameters, nozzle position, and air flow.

2.2.4.1. Cryogenic Machining

Cryogenic machining utilizes ultra-cold media like liquid nitrogen (LN_2) or liquid CO_2 for direct cooling. It effectively reduces temperatures, mitigates thermal wear, and extends tool life when cutting hard alloys. Subsequent research confirms its eco-friendly potential.

2.2.4.2. Cryogenic-MQL

Cryogenic-MQL combines MQL and cold air or cryogenic media, capitalizing on MQL lubricity and intense cryogenic cooling simultaneously.

2.2.5. Selection of Cooling Technology

From the above analysis, cooling and lubrication trends are shifting from traditional dry and flood cooling towards sustainable MQL-based techniques and hybrid MQL variants.

2.3. Design of Experiments and Methodology Selection

Based on these considerations, a blocked Box-Behnken response surface design was chosen to meet experiment count requirements, non-linear modeling capacity, and categorical factor handling. This design builds reliable predictive models, forming the basis for optimization in subsequent chapters. Detailed DOE parameters, input variables, and experimental matrices are presented in Chapter 3.

2.4. Modeling Methods

Modeling establishes quantitative relationships between input parameters and outputs such as surface roughness, force, and MRR. Models facilitate process prediction, parameter impact analysis, and optimization studies. Standard approaches encompass empirical regression and modern machine learning techniques.

2.4.1. Response Surface Methodology (RSM)

Response Surface Methodology (RSM) is a standard modeling technique in machining, establishing second-order polynomial regressions that describe input-output interactions.

2.4.2. Machine Learning Models in Machining

To overcome classical regression limitations, machine learning algorithms are applied to model machining. These models learn complex non-linear relationships from data without requiring predefined functional forms.

Among them, GPR is highly regarded for accurate predictions on small datasets while quantifying uncertainty.

2.4.3. Gaussian Process Regression (GPR)

Gaussian Process Regression (GPR) is a non-parametric Bayesian machine learning method where model outputs follow a Gaussian distribution. Instead of fitting a single curve, GPR defines probability distributions over functions using training data.

Key GPR advantages include strong non-linear modeling, robust performance with small samples, prediction confidence intervals, and kernel flexibility. These traits fit complex hard milling under nano-MQL, where input-output relationships exhibit pronounced non-linearity.

2.4.4. Model Evaluation and Selection

Comparative evaluation between models (e.g., RSM vs. GPR) identifies the best approach. GPR frequently yields superior accuracy over RSM in datasets with strong non-linearity or interaction effects.

2.4.5. Model Selection Summary

Each technique offers specific merits: RSM excels at preliminary screening and physical interpretations, whereas GPR delivers superior predictive performance in complex non-linear systems.

2.5. Optimization Methods

2.5.1. Single-Objective Optimization

Single-objective optimization determines input variables to optimize a target objective function. In hard milling, single-objective targets usually focus on: minimizing surface roughness (min Ra), maximizing material removal rate (max MRR), and minimizing cutting forces (min F).

2.5.2. Multi-Objective Optimization

In real machining processes, multiple target objectives often conflict,

e.g., increasing MRR elevates surface roughness, whereas lowering cutting forces restricts MRR.

Thus, Multi-Objective Optimization (MOO) is deployed to find trade-off solutions. Instead of a single point, MOO generates a Pareto optimal set, where no solution outperforms another across all objectives.

A Pareto optimal solution is defined as one where improving one objective degrades at least one other objective. The set of Pareto solutions forms the Pareto front, capturing objective trade-offs.

2.5.3. NSGA-II Algorithm

Non-dominated Sorting Genetic Algorithm II (NSGA-II) is widely used in multi-objective optimization due to high efficiency and robust global search capability.

NSGA-II advantages: Well-distributed Pareto set search, no objective weighting required, high computational efficiency, and seamless integration with predictive RSM or GPR models.

2.5.4. Combining Modeling and Optimization

Modern studies perform optimization on surrogate models (e.g., RSM or GPR) to cut computational and experimental costs. Algorithms like NSGA-II search surrogate domains to: minimize real experiments, accelerate computation, and thoroughly explore the design space.

2.5.5. Optimization Approach Summary

In this research, NSGA-II multi-objective optimization built upon GPR surrogate models is selected to establish the optimal Pareto set and guide machining regime selection in subsequent chapters.

Summary of Chapter 2

- Theoretical foundation: Analyzed chip formation, thermo-mechanical behavior, and key evaluation indicators (roughness, force, MRR).
- Lubrication technology: Selected nano-MQL as the optimal solution to improve friction and heat dissipation in the cutting zone.
- Experimental design: Applied blocked response surface methodology to optimize research variables.
- Modeling & Optimization: Employed RSM, GPR, and NSGA-II algorithms to predict and identify multi-objective optimal solutions.

CHAPTER 3: EXPERIMENTAL SYSTEM SETUP

3.1. Introduction

The experimental procedure consists of key steps: (i) setting machining conditions according to the DOE matrix; (ii) conducting machining on CNC milling machines under nano-MQL; (iii) collecting cutting forces, mass, and surface roughness data; (iv) storing and processing data for modeling and optimization. Overall schematics and procedures are detailed in subsequent chapter sections.

3.2. Machining Equipment and Experimental Setup

3.2.1. CNC Milling Center



Mazak VCS 530C Vertical Machining Center (Figure 3.1)

3.2.2. Kistler 9257BA Dynamometer



Figure 3.2: KISTLER 9257BA Force Measurement System

3.2.3 WT3003NE Electronic Balance



Figure 3.3: WT3003NE Electronic Balance

3.3. Cooling–Lubrication Conditions and Experimental Parameters

Nano-MQL was applied to improve tool-chip friction and zone heat dissipation. Key parameters include: Base oil: canola vegetable oil. Nanoparticles: copper oxide (CuO) at 2 wt.% concentration. Oil flow rate: 100 mL/h. Air pressure: 4 bar, ensuring stable aerosol atomization and uniform dispersion.

Four input variables were selected as independent factors in DOE: cutting speed v_c (m/min), feed per tooth f_z (mm/tooth), depth of cut a_p (mm), and average nanoparticle size D_avg (nm).

3.4. Description of Experimental Procedure

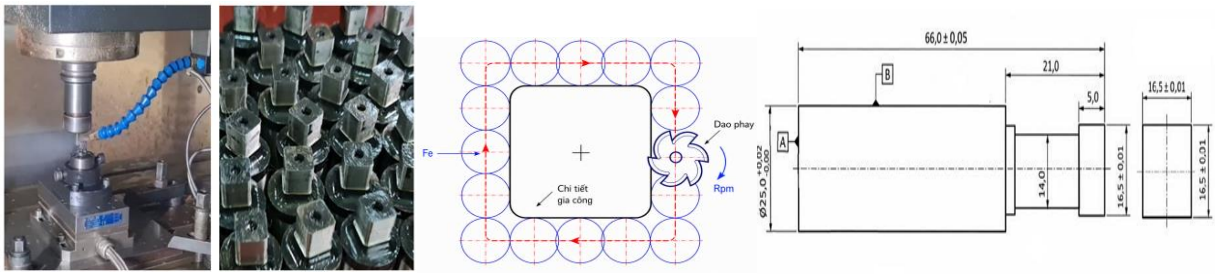


Figure 3.4: Experimental description and workpiece specimens: (a) CNC milling setup for external cylindrical hard milling of 90CrSi steel under nano-MQL (CuO); (b) Machined 90CrSi

steel specimens; (c) Machining trajectory diagram for external cylindrical forming; (d) Workpiece drawing

3.5.1. Process Variables and Categorical Factors

The primary technological parameters consist of three continuous variables: cutting speed (V), feed per tooth (F), and depth of cut (D), evaluated across three levels (low, center, high). Additionally, nanoparticle size (Sn) in lubricant serves as a discrete factor at 20, 50, and 100 nm.

3.5.2. Blocked Response Surface Design

To accommodate mixed factor types, a blocked response surface design was employed where each nanoparticle size defined an independent block. Within each block, tests were run with fixed Sn, isolating continuous factor effects (V, F, D) from systematic block variations.

3.5.3. Tool Diameter as a Discrete Variable and Data Collection Strategy

Milling cutter diameter was treated as a discrete input taking three values: Ø6mm, Ø9mm, and Ø12mm, corresponding to solid carbide nano-composite coated end mills manufactured by MOLDINO Tool Engineering, Ltd. (Japan).

3.5.4. Experimental Replications and Output Data Processing

Within each nanoparticle size block, design center points (V=125 m/min, F=0.03 mm/tooth, D=0.10 mm) were replicated three times, yielding nine center points per tool diameter. These center points allowed pure experimental error estimation and lack-of-fit testing for second-order response surface models per RSM guidelines [112].

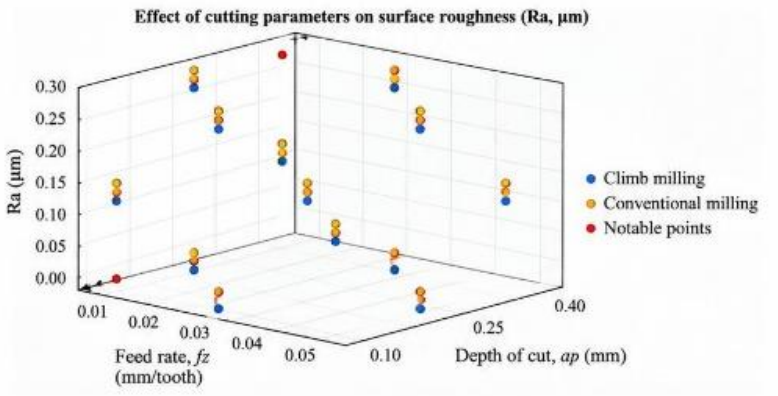


Figure 3.5. Geometric representation of blocked BBD design in spatial domain (v_c, f_z, a_p); colors indicate D_avg levels, while symbols represent test point types (edge centers, centers, and axial points).

3.5.5. Influence of Tool Diameter:

In this study, tool diameter was considered a discrete input (6 mm, 9 mm, 12 mm). To streamline testing and facilitate analysis, modeling, and comparisons, the four-variable DOE (v_c, f_z, a_p, D_avg) was executed independently for each tool diameter.

3.6. Measurement Methods and Output Responses

Primary output metrics for hard milling include surface roughness (Ra), cutting force (F), and material removal rate (MRR). These indicators thoroughly evaluate surface quality, mechanical load, and productivity. Measurement procedures are detailed as follows:

3.6.1. Surface Roughness Measurement (Ra)

Surface roughness (Ra) was measured using a Mitutoyo SJ-210 stylus profilometer. Measurements were recorded along the axial generator line of the cylindrical surface to capture geometric characteristics post-milling.

3.6.2. Cutting Force Measurement (F)

Cutting forces were recorded in real time using a Kistler 9257BA three-component dynamometer, capturing orthogonal force components F_x, F_y, F_z.

3.6.3. Determination of Material Removal Rate (MRR)

Material removal rate (MRR) evaluates machining productivity. Here, MRR was calculated massimetrically from pre- and post-machining workpiece weight differences measured on a high-precision WT3003NE balance.

Summary of Chapter 3

- Experimental System: Detailed CNC center, force measurement system, and precision weighing setup ensuring high accuracy.
- Cutting Conditions: Applied nano-MQL (CuO particles) on heat-treated 90CrSi tool steel workpieces.
- Experimental Design: Implemented a blocked Box-Behnken response surface methodology to optimize run numbers and statistical reliability.
- Output Measurement: Established measurement procedures and instrumentation for surface roughness, cutting forces, and MRR.

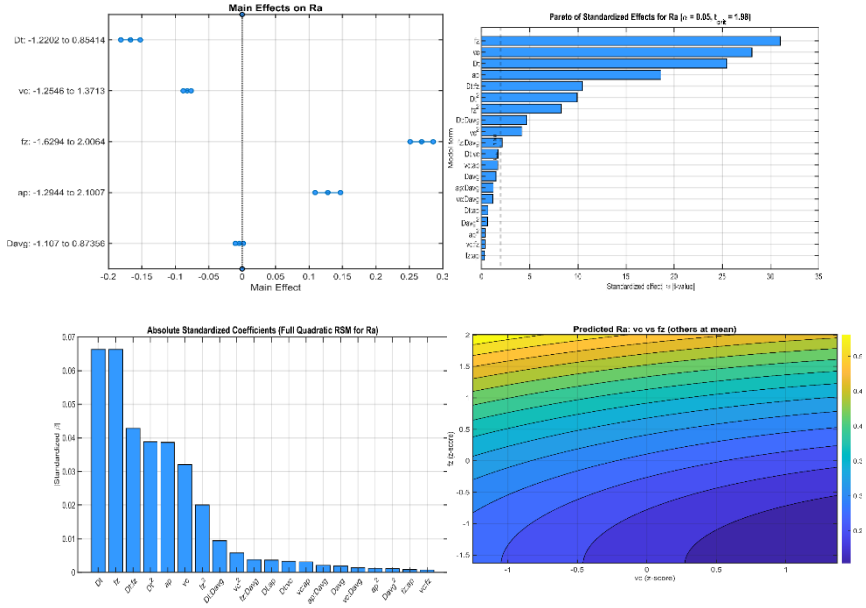
CHAPTER 4: EXPERIMENTAL RESULTS AND MODELING OF EXTERNAL CYLINDRICAL HARD MILLING OF 90CrSi STEEL UNDER NANO-MQL CONDITIONS USING CuO NANOPARTICLES

4.1. Experimental Results

Following experimental execution, the complete dataset—including input variables and output responses (Ra, MRR, F) for 90CrSi external cylindrical hard milling under nano-MQL with CuO nanoparticles—was compiled in Appendix 1. This experimental dataset forms the foundation for parameter effect analysis, predictive modeling, and optimization in subsequent chapter sections.

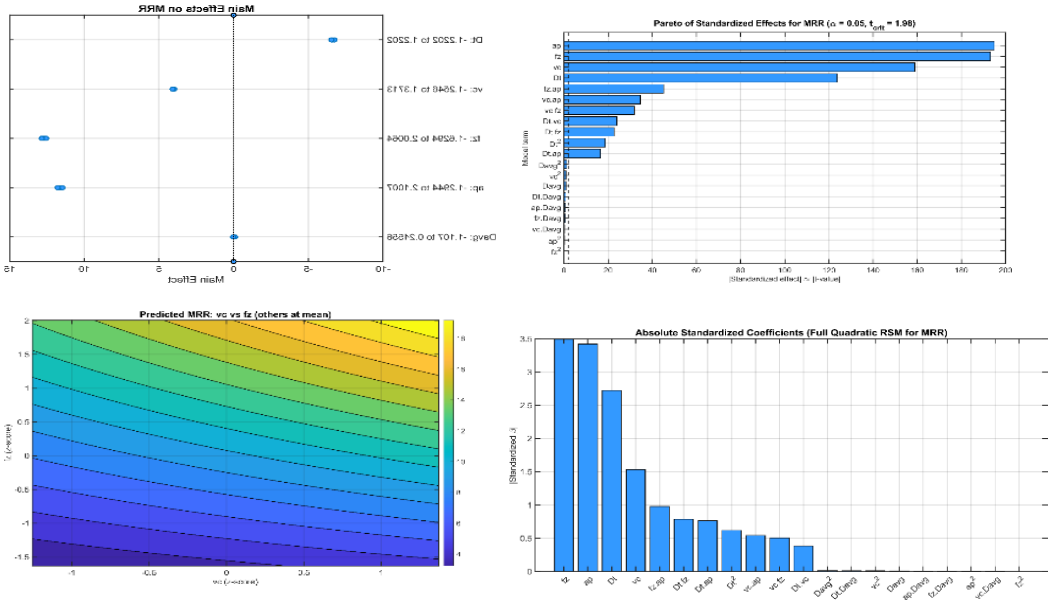
4.2. Analysis of Technological Parameter Effects

4.2.1. Effects on Surface Roughness (Ra)



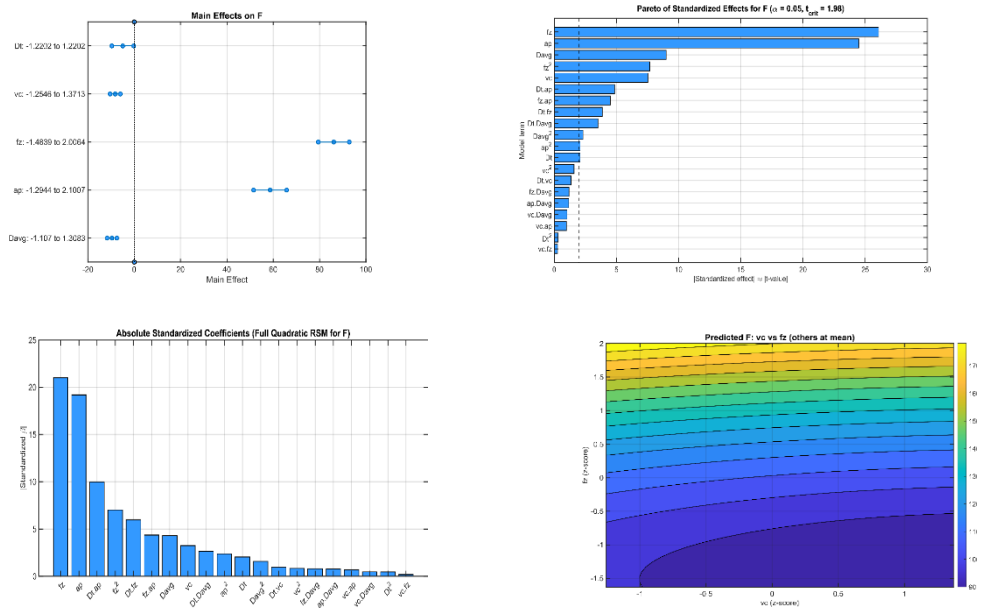
Summarizing the analysis indicates surface roughness in hard milling is primarily governed by feed per tooth and tool diameter, followed by depth of cut and cutting speed. Highly significant interaction and quadratic terms confirm that technological parameter relationships with Ra are non-linear and multivariate, requiring second-order response surface models for accurate process representation. Furthermore, the minor influence of nanoparticle size suggests it acts mainly in a supporting role via lubrication mechanisms rather than as a primary factor governing surface roughness.

4.2.2. Effects of Technological Parameters on Material Removal Rate (MRR)



This implies that for maximizing material removal productivity, optimizing cutting regime parameters is far more decisive than varying nanoparticle size in the nano-MQL fluid.

4.2.3. Effects of Technological Parameters on Cutting Force (F)



Therefore, to effectively control and minimize cutting forces, cutting regime factors, tool geometry, and nano-MQL conditions must be evaluated concurrently rather than isolating individual factors.

4.3. Analysis of Variance (ANOVA) for Models

Analysis of variance (ANOVA) was performed to evaluate statistical significance and adequacy of second-order RSM models constructed for three responses: surface roughness (Ra), material removal rate (MRR), and cutting force (F). Corresponding ANOVA results are summarized in Table 4.1, Table 4.2, and Table 4.3.

4.3.1. ANOVA for Surface Roughness Model (Ra)

Table 4.1. Analysis of variance (ANOVA) results for Ra model

Table 4.1. Analysis of Variance (ANOVA) Results for Surface Roughness (Ra)

Source	SS	DF	MS	F-value	P-value
Model	0.530606	20	0.026530	167.6007	1.15E-72
Milling strategy	0.460972	5	0.092074	582.8028	1.25E-78
Cutting speed × feed rate	0.048234	15	0.003216	19.3060	1.28E-24
Error	0.019085	114	0.000167	—	—
Lack-of-fit	0.018738	101	0.000186	9.6472	1.01E-05
Pure error	0.000350	13	0.000019	—	—
Total (corrected)	0.572594	134	0.004273	—	—

Note: Terms with P-values below 0.05 are statistically significant at the 95% confidence level.

4.3.2. ANOVA for Material Removal Rate Model (MRR)

Table 4.2. Analysis of Variance (ANOVA) Results for Material Removal Rate (MRR)

Source	SS	DF	MS	F-value	P-value
Model	2795.0572	20	139.7529	11345.6147	3.52E-178
Milling strategy	2613.7918	5	522.7584	42441.3701	2.12E-185
Cutting speed × feed rate	98.3810	15	6.1254	313.7093	4.05E-97
Error	1.3590	114	0.0119	—	—
Lack-of-fit	1.3062	101	0.0129	35.8654	3.86E-10
Pure error	0.0053	13	0.0004	—	—
Total (corrected)	2797.0203	134	20.8733	—	—

Note: Terms with P-values below 0.05 are statistically significant at the 95% confidence level.

4.3.3. ANOVA for Cutting Force Model (F)

Table 4.3. Analysis of Variance (ANOVA) Results for Cutting Force (F)

Source	SS	DF	MS	F-value	P-value
Model	173500.3333	20	8675.0167	364.5400	1.54E-143
Milling strategy	169136.5197	5	33827.3039	1426.2899	5.42E-185
Cutting speed × feed rate	4443.8139	15	296.2543	12.4812	8.77E-18
Error	2708.7386	114	23.7609	—	—
Lack-of-fit	2671.9638	101	26.4551	10.5000	1.53E-45
Pure error	31.2823	13	2.4063	—	—
Total (corrected)	176541.0714	134	1317.4707	—	—

Note: Values in this table should be checked against the original high-resolution table because some digits are difficult to read in the supplied image.

4.3.1.4. Comprehensive Assessment

Synthesizing ANOVA outcomes across all three models demonstrates that:

- All models demonstrate high statistical significance with p-values << 0.001
- Linear main effects exert dominant influence in all three responses
- Interaction and non-linear terms remain statistically significant, notably for Ra and MRR
- The MRR model exhibits the highest fit quality, followed by Ra and cutting force F
- Model error for F is slightly higher but remains well within acceptable limits for practical machining operations

In summary, constructed second-order RSM regression models are highly adequate, statistically significant, and reliable for interaction analysis and multi-objective optimization in subsequent sections.

4.4. Response Surface Modeling of Three Target Objectives

4.4.1. Modeling Objectives

Thus, the modeling objective extends beyond generating regression equations to establishing a robust modeling foundation capable of supporting analysis, prediction, and optimization in 90CrSi hard milling under nano-MQL with CuO nanoparticles.

4.4.2. Regression Model for Surface Roughness (Ra)

Based on pooled experimental data (Appendix 1), the second-order regression model for surface roughness Ra in actual units is formulated as follows:

$$\begin{aligned} Ra = {} & 0.848170 - 0.090865D_t - 0.005581v_c + 6.370997f_z + 1.461923a_p + 0.000633D_{avg} \\ & + 0.000070D_tv_c - 1.056083D_tf_z - 0.029585D_ta_p - 0.000115D_tD_{avg} \\ & - 0.002259v_cf_z - 0.003261v_ca_p - 0.000002v_cD_{avg} + 0.980891f_za_p \\ & + 0.006959f_zD_{avg} + 0.001262a_pD_{avg} + 0.006421D_t^2 + 0.000016v_c^2 \\ & + 73.515860f_z^2 - 0.472196a_p^2 + 0.000001D_{avg}^2 \end{aligned}$$

4.4.3. Regression Model for Material Removal Rate (MRR)

Based on pooled experimental data (Appendix 1), the second-order regression model for material removal rate MRR in actual units is formulated as follows:

$$\begin{aligned} MRR = {} & 0.933929 - 0.133226D_t - 0.011102v_c + 15.629736f_z - 1.171029a_p - 0.001525D_{avg} \\ & - 0.008220D_tv_c - 19.414208D_tf_z - 6.222731D_ta_p + 0.000150D_tD_{avg} \\ & + 1.615845v_cf_z + 0.571220v_ca_p - 0.000005v_cD_{avg} + 1184.490829f_za_p \\ & - 0.013207f_zD_{avg} - 0.004392a_pD_{avg} + 0.102578D_t^2 + 0.000030v_c^2 \\ & - 3.061537f_z^2 - 1.635751a_p^2 + 0.000016D_{avg}^2 \end{aligned}$$

4.4.4. Regression Model for Resultant Cutting Force (F)

Based on pooled experimental data (Appendix 1), the second-order response surface regression model for resultant cutting force F in actual units is formulated as follows:

$$F = 111.9446 - 7.7521D_t - 0.7521v_c + 938.9999f_z + 237.8213a_p - 0.0414D_{avg} + 0.0205D_tv_c - 147.3338D_tf_z + 81.1601D_ta_p - 0.0325D_tD_{avg} - 0.5946v_cf_z - 0.7218v_ca_p - 0.0007v_cD_{avg} - 5278.5399f_za_p + 1.4562f_zD_{avg} + 0.4555a_pD_{avg} + 0.0769D_t^2 + 0.0023v_c^2 + 25762.3114f_z^2 - 945.8464a_p^2 + 0.0014D_{avg}^2$$

Summary of Chapter 4

The study successfully constructed high-accuracy second-order RSM models for surface roughness, material removal rate, and cutting force during machining. Results demonstrate that feed rate, depth of cut, tool diameter, and CuO nanoparticles significantly affect output indicators, confirming model reliability for Chapter 5 optimization.

CHAPTER 5: OPTIMIZATION OF EXTERNAL CYLINDRICAL HARD MILLING OF 90CrSi STEEL UNDER NANO-MQL CONDITIONS USING CuO NANOPARTICLES

5.1. Single-Objective Optimization

5.1.1. Optimization Objectives and Methodology

Based on second-order RSM models developed in Chapter 4, three single-objective optimization problems were formulated to identify optimal cutting regimes for each primary output response. Specifically, optimization goals comprise:

Minimizing surface roughness Ra to achieve maximum surface finish quality;

Maximizing material removal rate MRR to enhance machining efficiency;

Minimizing resultant cutting force F to reduce mechanical loads and enhance process stability.

Objective functions are expressed as RSM regression models depending on input process variables:

$$f=f(Dt,vc,_z,ap,Davg) \quad (5.1)$$

5.1.2. Surface Roughness Optimization (Ra)

Surface roughness (Ra) min optimization is formulated according to the following equation:

$$\min f_0 Ra=f(Dt,vc,fz,ap,Davg) \quad (5.2)$$

Results indicate Dt and fz exert the strongest impact on Ra; increasing vc slightly decreases Ra owing to improved shear deformation; larger ap increases Ra; D_avg exhibits minor impact.

Optimal condition achieved: Dt=9 mm, Davg=100 nm, vc=150 m/min, fz=0.02 mm/tooth, ap=0.08 mm. Predicted value: Ra ≈ 0.144 μm, representing a fine and uniform finished surface.

5.1.3. Material Removal Rate Optimization (MRR)

Predicted optimal value achieved at: D_t=6 mm, D_avg=20 nm, v_c=150 m/min, f_z=0.08 mm/tooth, a_p=0.25 mm. Yielding MRR ≈ 42.06 g/min, representing high-productivity cutting conditions.

5.1.4. Resultant Cutting Force Optimization (F)

Optimal parameters identified: D_t=12 mm, D_avg=100 nm, v_c=141.2 m/min, f_z=0.023 mm/tooth, a_p=0.08 mm. Minimum cutting force reaches F ≈ 37.81 N, aligning with load reduction and tool life extension goals.

5.1.5. Experimental Validation

Table 5.1. Experimental validation results for single-objective optimal solutions

Objective	D_c (mm)	V□ (m/min)	fz (mm/tooth)	a_p (mm)	$D_{av}g$ (nm)	Predicted	Experimental	Error (%)
Minimum Ra (μm)	9	150	0.02	0.08	100	0.144	0.153	5.88
Maximum MRR (g/min)	6	150	0.08	0.25	20	42.06	40.32	4.14
Minimum F (N)	12	141.2	0.023	0.08	100	37.81	39.58	4.47

5.2. Theoretical Foundations of Multi-Objective Optimization and NSGA-II

5.2.1. Nature of Multi-Objective Optimization Problems

- Minimizing surface roughness (Ra) requires small feed rates and low depths of cut;
- Maximizing material removal rate (MRR) demands larger feed rates and deeper cuts;

These objectives cannot be simultaneously optimized at a single point, embodying the essence of Multi-Objective Optimization (MOO).

5.2.2. Pareto Set and Pareto Front Concepts

In this study, the Pareto front optimizes 3 criteria: Ra - MRR - F. Results display inverse trends: as Ra and F decrease, MRR increases more slowly or drops accordingly.

5.2.3. Multi-Objective Optimization Methods

In this research, NSGA-II (Non-dominated Sorting Genetic Algorithm II) was selected due to superior efficiency, stability, and solution diversity preservation.

5.2.4. NSGA-II Algorithm

NSGA-II, proposed by Kalyanmoy Deb [114], represents an enhanced Genetic Algorithm (GA) specifically engineered for multi-objective problems.

5.3. Multi-Criteria Decision-Making Methods

5.3.1. TOPSIS Method

TOPSIS (Technique for Order Preference by Similarity to Ideal Solution) is a multi-criteria decision-making (MCDM) method widely applied to rank optimal choices from feasible solution sets.

5.3.2. MARCOS Method

MARCOS (Measurement Alternatives and Ranking according to Compromise Solution) is an MCDM method developed to evaluate and rank alternatives based on relative utility relative to Ideal and Anti-Ideal Solutions.

5.3.3. EAMR Method

EAMR (Evaluation by an Area-based Method of Ranking) is an MCDM technique evaluating and ranking alternatives according to integrated criterion evaluation values.

5.4. Formulation of Multi-Objective Optimization via NSGA-II

5.4.1 Input Variables and Target Objective Functions

Three target objectives considered simultaneously include:

Surface roughness (Ra) - to be minimized to enhance surface quality and meet technical part specifications.

Resultant cutting force (F) - to be minimized to decrease tool, fixture, and machine loads, enhancing process stability and tool life

Material removal rate (MRR) - to be maximized to improve machining productivity and manufacturing economic efficiency.

Table 5.2. Input variables and domain ranges utilized in multi-objective optimization.

Symbol	Machining parameter	Unit	Search range
D_t	Tool diameter	mm	(6, 9, 12)
V□	Cutting speed	m/min	100–150
fz	Feed per tooth	mm/tooth	0.02–0.04
a_p	Depth of cut	mm	0.08–0.12
D_{avg}	CuO nanoparticle size	nm	(20, 50, 100)

5.4.2. Technological Constraints

$$\begin{cases} 100 \le v_c \le 150 \\ 0.02 \le f_z \le 0.04 \\ 0.08 \le a_p \le 0.12 \end{cases} \quad (5.9)$$

Bên cạnh đó, D_t và D_{avg} là luôn lấy các giá trị nguyên và mỗi biến chỉ có 3 giá trị. Cụ thể (5.8):

$$D_t \in \{6, 9, 12\} \text{ và } D_{avg} \in \{20, 50, 100\} \quad (5.10)$$

5.4.3. Conversion and Standardization of Optimization Directions

Following optimization completion, MRR values were converted back to original form to analyze, compare, and assess technological implications of obtained Pareto solutions.

5.4.4. NSGA-II Parameter Settings

Parameter	Value	Notes
MaxIt	120	Number of generations
nPop	60	Population size
pCrossover	0.90	Crossover probability
nCrossover	54	Number of crossover offspring = 2 × round(pCrossover × nPop / 2)
pMutation	0.25	Mutation probability
nMutation	15	Number of mutation offspring = round(pMutation × nPop)
mu	0.03	Mutation probability for each variable
Mutation step	0.1 × (VarMax – VarMin)	Gaussian mutation step
logEvery	10	Display interval: every 10 generations
nSnapshots	4	Number of generations used to illustrate the evolution of the Pareto front
hvMC Samples	2×10^5	Number of Monte Carlo samples for 3D hypervolume calculation
rng seed	2025 (twister)	Random-number generator seed
Number of design variables	5	Dt, Vc, fz, ap, Davg
Discrete variables	Dt, Davg	Selected from discrete candidate values
Search domain	Minimum–maximum based on experimental data	Bounded by the minimum and maximum values in the experimental dataset
Objective functions	MRR, Ra, F	Maximize MRR; minimize Ra and F

5.4.5. NSGA-II Optimization Workflow

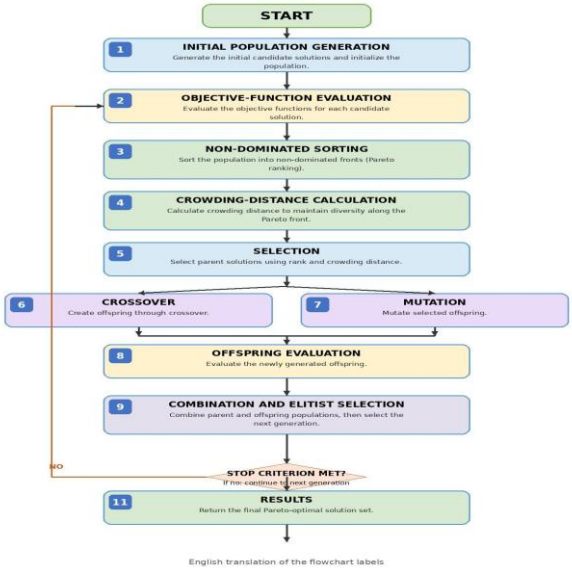


Figure 5.1: NSGA-II flowchart applied to the multi-objective optimization problem

5.4.6. Identification of Knee Point on Pareto Front

This approach identifies the solution exhibiting the most pronounced trade-off among material removal rate (MRR), surface roughness (Ra), and resultant force (F), aligning with Das's Knee concept [116]. The obtained Knee point serves as a reference benchmark to compare against TOPSIS, MARCOS, and EAMR choices in discussion sections.

5.5. Results and Discussion

5.5.1. Accuracy Evaluation of GPR Models

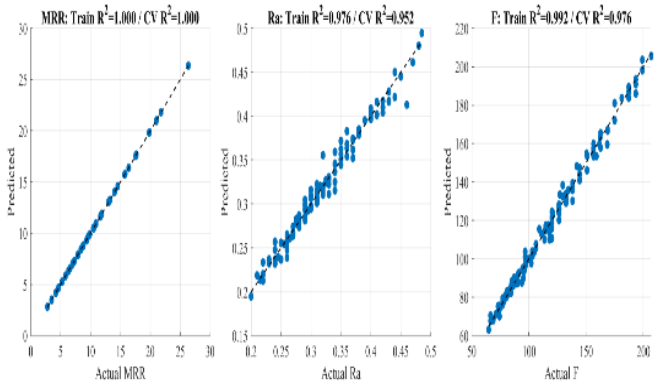


Figure 5.2. Comparison between predicted and experimental values for GPR models of MRR, Ra, and F.

Data points in Figure 5.2 align closely along the ideal 45° line, proving small prediction errors and excellent generalization capability of GPR models. Consequently, GPR models are deemed dependable surrogate models for NSGA-II multi-objective optimization.

5.5.2. Convergence Analysis of NSGA-II Algorithm

Convergence of NSGA-II was evaluated using the Hypervolume (HV) metric, as plotted in Figure 5.3.

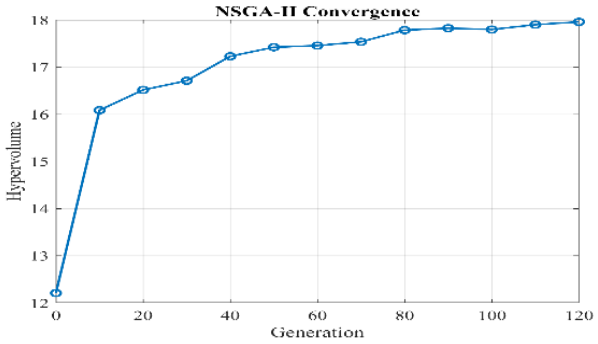
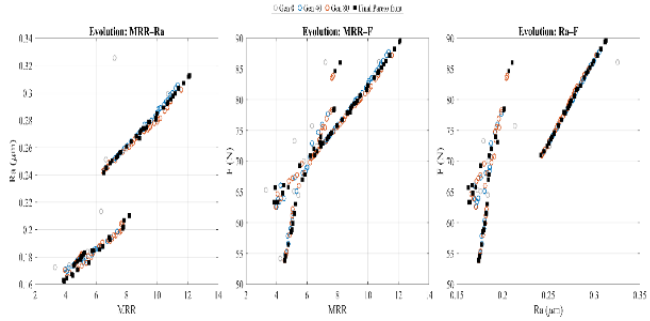


Figure 5.3. Hypervolume metric progression versus evolutionary generation count in NSGA-II.

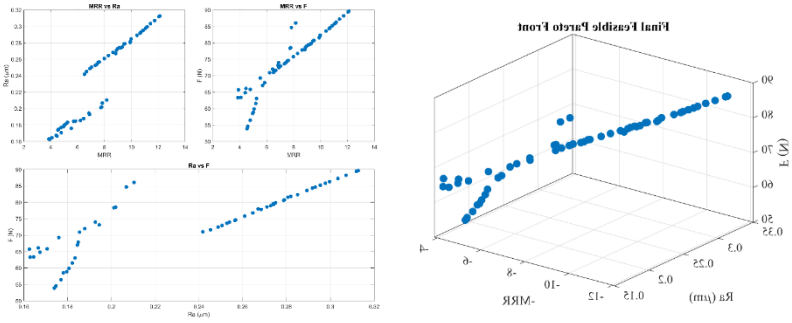
5.5.3. Evolution of the Pareto Solution Set

The evolutionary progression of the Pareto set is depicted in Figure 5.4.



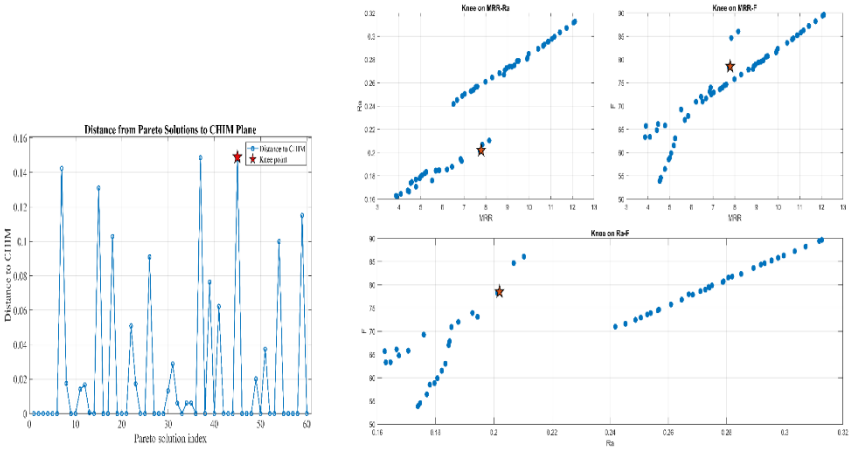
5.5.4. Analysis of Final Pareto Solution Set

The final Pareto set obtained via NSGA-II is plotted in 3D objective space in Figure 5.5 and 2D projections in Figure 5.6.



5.5.5. Analysis of Knee Point on Pareto Front

The Knee point corresponds to the Pareto solution exhibiting maximum perpendicular distance to the CHIM plane in normalized objective space. Results are illustrated in Figure 5.7 and Figure 5.8.



5.5.6. Selection of Optimal Solution via MCDM Methods

Notably, all three MCDM methods converged on the identical optimal solution (Option 21). Absolute consensus among TOPSIS, MARCOS, and EAMR demonstrates high solution stability while positioning close to ideal solutions in multi-objective space. This highlights decision-making consistency when applying diverse MCDM algorithms across the feasible Pareto front.

5.5.7. Selection of Optimal Solution for Industrial Practice

The selected solution across all three MCDM methods specifies cutting parameters: Dt = 9 mm, vc = 148.11 m/min, fz = 0.038 mm/tooth, ap = 0.11 mm, and Davg = 100 nm. Predicted responses achieve MRR = 6.89 g/min, Ra = 0.19 µm, and F = 73.97 N.

5.5.8. Experimental Validation

Machining parameters used in validation testing were Dt=9 mm, vc=148.11 m/min, fz=0.038 mm/tooth, ap=0.11 mm, and Davg=100 nm. Predicted response values for MRR, Ra, and F were obtained from GPR models and compared against experimental measurements. Comparative results are shown in Table 5.8.

Table 5.8. Comparison of Predicted and Experimental Values at the Selected Optimal Machining Conditions

Objective	Predicted value	Experimental value	Error (%)
MRR (g/min)	6.89	6.78	1.60
Ra (µm)	0.19	0.18	5.26
F (N)	73.97	71.24	3.68

Summary of Chapter 5

Chapter 5 successfully applied GPR models to accurately predict MRR, Ra, and F responses. The NSGA-II algorithm executed multi-objective optimization, establishing a stable converged Pareto front. After excluding the Knee point due to industrial constraint mismatches, three MCDM methods (TOPSIS, MARCOS, EAMR) unanimously identified a single practical optimal machining regime. Experimental validation at this regime demonstrated error below 6% relative to theoretical predictions, confirming high model reliability and practical significance.

CONCLUSIONS AND RECOMMENDATIONS

1. Conclusions

•Experimental setup: A milling system was successfully configured for external cylindrical machining of 90CrSi steel using nano-MQL (CuO) cooling/lubrication. The experiments were conducted according to the Box–Behnken design.

•Observed relationships: Feed per tooth and depth of cut strongly affect MRR and cutting force; feed per tooth and CuO nanoparticle size affect surface roughness.

•Modeling: Second-order RSM models and a GPR machine-learning model were developed, providing high accuracy and reliable predictions.

•Optimization: NSGA-II was used to identify a stable Pareto front. The Knee Point method was excluded because the selected solution did not satisfy the criterion $Ra \leq 0.2$ μm.

•Decision-making: The MCDM methods TOPSIS, MARCOS, and EAMR jointly selected a single optimal machining condition: Dt = 9; Vc = 148.11; fz = 0.038; ap = 0.11; Davg = 100.

•Validation: The experiment conducted at the selected optimum had an error belw 6%, supporting the accuracy of the model.

•Significance: An integrated workflow combining experiments, GPR, NSGA-II, and MCDM is proposed, with scientific and practical value for machining.

2. Future Research Directions

-Workpiece and lubricant materials: Extend the investigation to other nanoparticle types or nanofluids.

-Optimal concentration: Further investigate the effect of CuO nanoparticle concentration on machining quality and productivity.

-Evaluation criteria: Include cutting-zone temperature, tool wear, residual stress, and surface-integrity measurements.

-Hybrid technologies: Integrate nano-MQL with ultrasonic vibration, cold-air cooling, or cryogenic-MQL.

-Modeling and sustainability: Develop machine-learning (AI) models and incorporate energy efficiency, cost, and sustainable-manufacturing criteria.